EXPLORATORY WIND-TUNNEL INVESTIGATION OF THE EFFECT OF THE MAIN ROTOR WAKE ON TAIL ROTOR NOISE

Robert J. Pegg and Phillip A. Shidler
NASA Langley Research Center

SUMMARY

One of the primary sources of noise from a helicopter is the noise of the tail rotor. To a large extent, the intensity of this noise is affected by the interaction of the tail rotor blades with the wake of the main rotor. Under most flight conditions the flow from the main rotor is very turbulent and unsteady and results in higher levels of tail rotor noise than that which would normally occur from the tail rotor operating in an undisturbed flow. This increase in tail rotor noise apparently arises from ingestion of the main rotor non-uniform wake into the tail rotor and the interactions of the main rotor tip vortices with the tail rotor blades.

Approaches to minimizing this interaction noise have included re-positioning of the tail rotor with respect to the main rotor, changes in the rotational direction of the tail rotor, and modification of the main rotor tip vortex. No straight-forward solution, however, exists for all situations.

In view of the complexity of the problem of main rotor/tail rotor interactions and lack of suitable analytical techniques to study the problem in detail, an experimental program was conducted in order to further the understanding of this noise phenomenon.

A variable geometry model was built which had the capability of varying tail rotor position relative to the main rotor as well as direction of tail rotor rotation. Acoustic data taken from the model in the Langley anechoic noise facility indicates interaction effects due to both the main rotor shed vortex and the main rotor turbulence.

INTRODUCTION

For the vast majority of helicopters flying today torque compensation and directional control is accomplished by means of a tail rotor. Although the tail rotor produces less thrust and consumes less power than the main rotor, it can be a serious source of noise since its harmonics usually predominate in the frequency range from 200 Hz to 3000 Hz.

References 1, 2, and 3 detail some operational problems and design considerations which are involved in current tail rotor design procedures. In addition to these requirements, constraints are being considered to have helicopters conform to governmental noise regulations.

The intensity of the tail rotor noise is affected by the interaction of the tail rotor blades with the wake of the main rotor. Under most flight conditions the ingested flow from the main rotor is very turbulent and unsteady and results in higher levels of tail rotor noise than would occur normally if the tail rotor were operating in undistrubed flow. Reference 4 discusses the results of a test program with a production helicopter in which significant noise reduction was achieved by reversing the direction of the tail rotor rotation. Because of the numerous other constraints (refs. 1, 2, and 3) placed on the tail rotor design, no straight-forward solution to the noise problem exists for all operational situations. Tail rotor noise problems, however, were treated analytically by Levine in reference 5 for a large helicopter. A wind-tunnel model was built and a preliminary experimental program was conducted in order to further the understanding of this noise phenomenon. The intial effort is reported in reference 6. The focus of the present investigation is to extend the work of reference 6 and to provide an insight into the flow mechanism causing the interaction noise.

INTERACTION NOISE MECHANISM

The tail rotor on most conventional helicopters is subjected to a highly turbulent and unsteady flow environment which has the potential to produce noise levels that would not be present in a quiescent flow. This excess noise is in addition to rotational and broadband noise gathered by free rotor. Specifically, the tail rotor disk is immersed totally or partially in the main rotor wake during most flight conditions and is influenced by whatever installation effects are found for a particular design (i.e., effect of tail rotor fin on tail rotor inflow). The water tunnel flow studies of reference 7 provide an indication of the flow environment at the tail rotor. This wake disturbance is comprised of two principal ingredients: the shed vortices from the main rotor and the random turbulent wake lying between the upper and lower vortex boundaries. Figure 1 illustrates a cross-section of the complex flow field in which the tail rotor operates. As outlined in reference 8, the effect of the random, non-uniform part of the inflow on the tail rotor noise is to increase the level of the discrete tones at blade passage frequency as a result of non-uniform blade loading. Both reference 4 and reference 6 indicate that discrete frequencies which are not multiples of the tail rotor rotational speed are also produced.

The noise resulting from the interaction of the blades with the shed tip vortices of the main rotor is characterized by discrete tones occurring at combination frequencies which are nTR ± mMR. MR and TR are blade passage frequencies of the main and tail rotors and n and m are harmonic integers. Depending on the number of tail rotor blades and the flight condition, a blade may intersect a vortex several times before it passes through the tail rotor disk.

In order to examine the interaction noise in detail, it is necessary to determine how the main rotor wake intersects the tail rotor. This can be done by using a free-wake analysis to predict accurate vortex trajectories. This technique,however, requires considerable computer time to obtain a satisfactory answer (ref. 9.) A simplified approach to the tip vortex trajectory problem can be obtained from the modified momentum analysis of Coleman in reference 10. This simplified approach does not account for wake instabilities or rotor disk leading edge lap-over that has been observed on helicopters under actual flight conditions. It is assumed, however, that the wake distortion in forward flight at the tail rotor position is of second order importance because of the close proximity of the tail rotor to the main rotor. The following equations have been used to determine the fore and aft wake trajectory boundaries adjacent to the main rotor:

wake trajectory at center of rotor:

$$\text{Tan}\ \chi_o = -\frac{\mu}{\lambda_0} \tag{1}$$

where:

χ_o is the wake angle at the center of the rotor; μ is the advance ratio and λ_0 is the inflow ratio at the rotor center.

Induced velocities at the leading and trailing edge of the rotor disk:

$$w = w_o(\pm\tan\ \chi_o/2) \tag{2}$$

where:

w_o is the induced velocity at the center of the rotor disk. The positive sign indicates the induced velocity from the aft portion of the disk.

The fore and aft wake angles are:

$$\tan\ \chi_F = -\frac{V_F\cos\alpha}{V_F\sin\alpha - w_F} \tag{3a}$$

$$\tan\ \chi_R = -\frac{V_F\cos\alpha}{V_F\sin\alpha - w_R} \tag{3b}$$

where:

V_F and α are the forward velocity and rotor angle of attack, respectively.

Figure 2 shows the calculated wake trajectories for the six different forward flight operating conditions used in this program.

MODEL TEST PROGRAM

The tests were conducted in the Langley anechoic noise facility and were planned as the initial phase of a detailed program to reduce tail rotor noise. This section of the paper describes the helicopter model, the test setup, and the data acquisition and reduction procedures.

Helicopter Model

A photograph of the model used for this investigation is shown in figure 3. The model uses a two-bladed rotor system with offset flapping hinges. The two main rotor blades have a radius of 59.06 cm (18.0 in.), a 4.45 cm (1.36 in.) chord, and a -8° linear twist from blade root to blade tip. The blades have an NACA 0015 airfoil section. Flapping hinge offset from the center of rotation is 1.92 cm (0.756 in.) or 4.2 percent of the radius. The two-bladed tail rotor is 19.1 cm (7.5 in.) in diameter and has a chord of 1.14 cm (0.45 in.). The untwisted tail rotor blade has an NACA 0015 airfoil section and is cantilevered to the hub. The spacing between the fin and the tail rotor is approximately 1.3 cm (0.5 in.) Both the main and tail rotors have square blade tips.

The helicopter model was designed in such a manner as to provide the capability for variations in the main rotor wake/tail rotor operating parameters (fig. 3). The design features of the model which provided this flexibility are: (a) adjustable tail boom length, (b) adjustable tail boom angle, (c) variable tail rotor rotational speed, (d) direction of the tail rotor rotation, (e) direction of tail rotor thrust, (f) variation of main rotor thrust and rotational speed, and (g) variation in model angle of attack. Table I lists the range over which these parameters could be varied. The model was operated such that the tail rotor downwash was against the fin and that the advancing blade was in the upper portion of the disk.

The helicopter model is provided with two electric motors. A 2.2-kw (3 hp), 220-V, 60-Hz motor powers the main rotor. A 0.003 kw (0.004 hp) motor drives the tail rotor. Rotational speed on both motors can be varied from 0 to a maximum of 4400 rpm on the main rotor drive and 13,000 rpm on the tail rotor. Load measuring devices around the main rotor shaft and at the base of the tail boom are used to measure the main and tail thrust.

Wind-Tunnel Tests

The wind-tunnel tests were conducted in the Langley anechoic noise facility. Figure 4 is a schematic diagram of the microphone positions with respect to the model. Tunnel speeds for the tests were 0.0, 10.0, 20.1, and 29.8 m/sec resulting in advance ratios of 0, 0.10, 0.20, and 0.29, respectively, at a nominal main rotor rotational speed of 2120 rpm. A summary of the test conditions and model configurations are presented in Table I. Tests were conducted with the model both in and out of trim, these conditions are shown in figure 5 as a function of main rotor blade setting and tunnel velocity. Also given are the vortex circulation values, Γ, for each operating point.

Typical background noise levels are shown in a narrow band presentation to 5000 Hz for the four test velocities in figure 6. These spectra were obtained with the model in place and with the rotors stopped. These background noise levels are shown below the measured data. The tones which appear in the spectra are apparently due to vortex shedding from the model.

Data Acquisition and Reduction

The noise measurement equipment used for these tests was a commercially available system. Four free-field microphones were used in the test program. These microphones are condenser types having a 1.27 cm (0.5 in.) diameter active diaphram and a frequency response that was flat to within ± 1½ dB over the frequency range from 5 to approximately 15 000 Hz. An FM magnetic tape recorder was used to record the microphone output for these tests. The response was flat within ±3 dB from 0 to 10 000 Hz at 38 cm/sec (15 ips) tape speed with wide band recording. All acoustic measurements were made in accordance with the recommendation of reference 11. The entire sound measurement system was calibrated immediately before and after the tests by means of a discrete-frequency calibrator. A 100 Hz high-pass filter was used to obtain greater dynamic range. The data of interest in this investigation is all well above the 100 Hz cutoff frequency.

The data obtained from these tests were reduced by analog methods. Narrow band analyses were made using a spectrum analyzer. The resultant spectra cover a range from 0 to 2000 Hz with a 12 Hz resolution and from 0 to 5000 Hz with a 30 Hz resolution.

TEST RESULTS

The test program discussed in this paper is the first phase of a more extensive investigation into tail rotor noise due to interaction effects. The results will be presented to illustrate the acoustic characteristics of the basic helicopter model and the effects of the interaction. The data will be in the form of sound pressure time histories and acoustic spectra. figure 7 illustrates a typical acoustic time history of the complete model and a corresponding spectrum. The tail rotor harmonics and tail rotor/fin tones are identifiable. This is an installation effect and is due to the momentary disturbance of the uniform loading of the tail rotor by the presence of the fin.

No-flow Interaction Effects

A typical acoustic spectrum of the main and tail rotors alone and also together are shown in figure 8. The tunnel velocity for this condition is zero and for this particular case data were taken from microphone 2. There was no ground plane used during these hover tests. The main rotor was lightly loaded as is indicated by the circulation value in figure 5. The discrete tones of the tail rotor have been identified and are the maximum levels as marked by the circles. The broadband noise floor level is below the dynamic range of the recording system. The acoustic spectrum for the main rotor alone is given with the solid lines. Harmonics are discernable to the 21st blade passage frequency. The broadband noise floor for the main rotor varies from approximately 50 dB to 55 dB.

For the hover flight condition, the interaction appears to affect the noise of the main rotor. Although the fundamental and first few harmonics do not change when the main and tail rotors are operated together, there is a definite increase in the higher order main rotor harmonics. No appreciable changes are noted in the tail rotor harmonics. This phenomenon is probably due to the local velocity field around a small portion of the main rotor induced by the tail rotor.

Interaction Effects With Tunnel Flow

The effect of forward speed on the source of the interaction noise, namely the main rotor wake, is to skew the wake into the tail rotor beginning at very low speeds. The calculated wakes are shown schematically in figure 2. The effect of increased forward speed at different tail positions is shown in figures 9 and 10 for 10 and 20-m/sec. From the data of these figures it can be seen that combination tones are present that have frequencies nTR ± mT[illegible] These tones are generated by the intersection of shed main rotor vortices and the tail rotor blades. As a vortex passes through the tail rotor disk, it may intersect each blade at different radial stations depending on the blade azimuth. An intersection on an advancing blade tip will produce a stronger impulsive type loading than one farther down the blade because of the relative velocities of the blade and vortex and the short duration of the encounter. Numerous intersections can be made as the vortex passes through the tail rotor disk.

A comparison of the acoustic pressure time histories in Figure 11 indicates a progression of events. The sound pressure time history at 10 m/sec and low tail rotor position clearly shows the passage of the tail rotor blade; however, as the tunnel velocity is increased to 29.8 m/sec, the tail rotor modulated pressure signal is overshadowed by the individual blade-vortex intersections. At the higher tail rotor position the impulsive character of these intersections are somewhat reduced but are still the prevalent noise source.

The effect of inflow turbulence on the acoustic spectra to 5,000 Hz is shown in figure 12. For the tail rotor in the raised position and 29.8 m/sec tunnel velocity, significant tones at tail rotor blade passage frequency occur between 2000 Hz and 5000 Hz. This phenomenon was noted only in this operating condition.

CONCLUDING REMARKS

A research program has been initiated to investigate the aero/acoustic mechanisms relating to the increased tail rotor noise from the influence of the main rotor. This paper discusses the results of the first phase of this program. The helicopter model with a 118 cm (3 ft) diameter main rotor was used in the investigation. This model can vary tail rotor position with respect to the main rotor, tail rotor speed and thrust direction and overall model and wake orientation. In general, it was shown that a model of this size had.the capability of providing information relative to the mechanisms involved in interaction noise and thus is a tool to explore techniques for reducing this noise source.

During the investigation it was found that certain characteristics of tail rotor noise were attributable to the interaction effects of the main rotor wake turbulence and shed vortices and certain installation effects. Interaction effects are hypothesized to originate from the intersection of the tail rotor baldes with the shed main rotor vortices and turbulent main rotor wake. These sources create additional tones which are combinations of the main and tail rotor frequencies as well as increasing the level of existing tail rotor harmonics. The primary installation effect is due to the asymmetric loading on the tail rotor disk due to a tail rotor blade passing over the tail fin. This effect produces acoustic harmonics which, under uniform loading conditions would cancel completely in the disk.

During hover conditions, the main rotor noise reflected an interaction effect on the tail rotor on the main rotor flow field. Although the first several main rotor acoustic harmonics did not change in amplitude, the higher main rotor harmonics were increased as well as the level of the broadband noise floor.

REFERENCES

1. Lynn, R. R.; Robinson, F. D.; Batra, N. N.; and Duhon, J. M.: Tail Rotor Design. Part I: Aerodynamics. J. American Helicopter Soc., Vol. 15, no. 4, Oct. 1970, pp. 2-15.

2. Sheridan, Philip F.; and Wiesner, Wayne: Aerodynamics of Helicopter Flight Near the Ground. Preprint No. 77.33-04. Presented at 33rd Annual Nat. Forum of the American Helicopter Soc., May 1977.

3. Wiesner, Wayne; and Kohler, Gary: Tail Rotor Performance in Presence of Main Rotor, Ground, and Wings. J. American Helicopter Soc., Vol. 19, No. 3, July 1974, pp. 2-9.

4. Leverton, John W.; Pollard, John S.; and Willis, Christopher R.: Main Rotor Wake/Tail Rotor Intersection. Vertica, Vol. 1, 1977, pp. 213-221.

5. Levine, Larry S.: An Analytic Investigation of Techniques to Reduce Tail Rotor Noise. NASA CR-145014, 1976.

6. White, Richard P.; Balcerak, John C.; and Pegg, Robert J.: A Parametric Model Study of the Noise Generated by the Aerodynamic Interaction of the Tail Rotor with the Wake of the Main Rotor. American Helicopter Soc. Mid-East Region Symposium on Rotor Technology. Essington, Pa., Aug. 1976.

7. Lehman, August F.: Model Studies of Helicopter Tail Rotor Flow Patterns In and Out of Ground Effect. USAAVLABS TR 71-12, April 1971.

8. Hayden, Richard R.: Some Advance in Design Techniques for Low Noise Operation of Propellers and Fans. Presented at Noise-Con 77 (Hampton, Va.), Oct. 1977.

9. Sadler, S. Gene: Development and Application of a Method for Predicting Rotor Free Wake Positions and Resulting Rotor Blade Air Loads. NASA CR-1911, Dec. 1971.

10. Coleman, Robert P.; Feingold, Arnold M.; and Stempin, Carl W.: Evaluation of the Induced-Velocity Field of an Idealized Helicopter Rotor. NACA WR L-126, 1945. (Formerly NACA ARR L5E10.)

11. Measurements of Aircraft Exterior Noise in the Field. ARP796, Soc. Automotive Eng., Inc., June 15, 1965.

TABLE I.- SUMMARY OF NOMINAL OPERATING CONDITIONS

[θ_m, main rotor blade pitch; θ_T, tail rotor blade pitch; α_e, model angle of attack; ℓ_t, boom extension; α_B, boom angle]

Run	Rotor speed, rpm		Tunnel conditions		Model configuration				
	Main	Tail	Speed, m/sec	Temp., °C	θ_m, deg	θ_T, deg	α_e, deg	$\Delta\ell_t$, cm	α_B, deg
Untrimmed conditions									
1	0	0	10	26.7	----	---	-----	-----	-----
2	0	0	20	26.7	----	---	-----	-----	-----
3	0	0	29.8	26.7	----	---	-----	-----	-----
4	2120	0	10	27.2	11.5	5	-8	10.67	-19.3
5	2120	0	20	27.2	11.5	5	-8	10.67	-19.3
6	2120	0	29.8	27.8	11.5	5	-8	10.67	-19.3
7	0	10 800	10	29.4	11.5	5	-8	10.67	-19.3
8	0	10 800	20	29.4	11.5	5	-8	10.67	-19.3
9	0	10 800	29.8	30.6	11.5	5	-8	10.67	-19.3
10	2120	10 800	10	30.0	11.5	5	-8	10.67	-19.3
11	2120	10 800	20	30.0	11.5	5	-8	10.67	-19.3
12	2120	10 800	29.8	30.0	11.5	5	-8	10.67	-19.3
13	2120	10 800	10	30.0	11.5	5	-8	10.67	+4
14	2120	10 800	20	30.0	11.5	5	-8	10.67	+4
15	2120	10 800	29.8	30.6	11.5	5	-8	10.67	+4
16	2120	10 800	10	29.4	11.5	5	-8	23.37	+4
17	2120	10 800	20	30.0	11.5	5	-8	23.37	+4
18	2120	10 800	29.8	30.6	11.5	5	-8	23.37	+4
19	2120	10 800	10	30.6	11.5	5	-8	17.02	+4
20	2120	10 800	20	30.6	11.5	5	-8	17.02	+4
21	2120	10 800	29.8	30.6	11.5	5	-8	17.02	+4
22	2120	10 800	10	27.8	11.5	5	-8	10.67	-.2
23	2120	10 800	20	27.8	11.5	5	-8	10.67	-.2
24	2120	10 800	29.8	28.3	11.5	5	-8	10.67	-.2
25	2120	10 800	10	28.3	11.5	5	-8	17.02	-.2
26	2120	10 800	20	28.3	11.5	5	-8	17.02	-.2
27	2120	10 800	29.8	28.3	11.5	5	-8	17.02	-.2
28	2120	10 800	10	28.9	11.5	5	-8	17.02	-.2
29	2120	10 800	20	28.3	11.5	5	-8	23.37	-.2
30	2120	10 800	29.8	28.3	11.5	5	-8	23.37	-.2
31	2120	10 800	10	28.9	11.5	5	-8	23.37	-19.3
32	2120	10 800	20	28.9	11.5	5	-8	23.37	-19.3
33	2120	10 800	29.8	28.9	11.5	5	-8	23.37	-19.3
34	2120	10 800	10	28.9	11.5	5	-8	23.37	-19.3
35	2120	10 800	20	28.9	11.5	5	-8	23.37	-19.3
36	2120	10 800	29.8	28.9	11.5	5	-8	23.37	-19.3
Trim conditions									
1	2120	0	0	26.1	11.5	5	-8	14.48	-19.3
2	0	10 800	0	26.1	11.5	5	-8	14.48	-19.3
3	2120	10 800	0	26.1	11.5	5	-8	14.48	-19.3
4	2120	10 800	10	26.7	14.5	4.1	-2.3	14.48	.2
5	2120	10 800	10	27.2	14.5	4.1	-2.3	14.48	3.8
6	2120	10 800	10	27.2	14.5	4.1	-2.3	14.48	-19.3
7	2120	10 800	20	27.2	14.3	2.7	-5.6	14.48	-19.3
8	2120	10 800	20	28.3	14.3	2.7	-5.6	14.48	.2
9	2120	10 800	20	28.9	14.3	2.7	-5.6	14.48	3.8
10	2120	10 800	29.8	30.0	15.9	3.2	-10.0	14.48	3.8
11	2120	10 800	29.8	30.0	15.9	3.2	-10.0	14.48	.2
12	2120	10 800	29.8	30.6	15.9	3.2	-10.0	14.48	-19.3

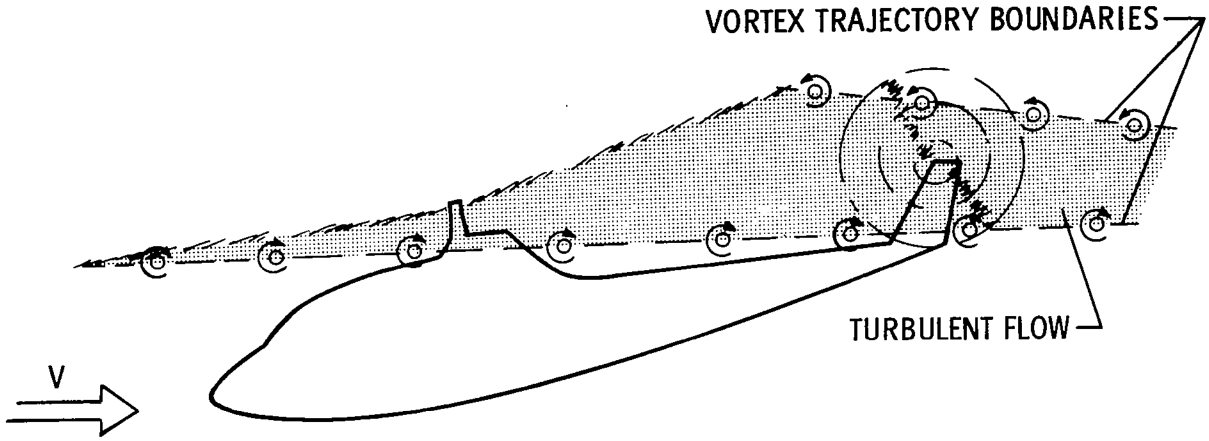

Figure 1.- Cross-section of main rotor wake disturbances on tail rotor.

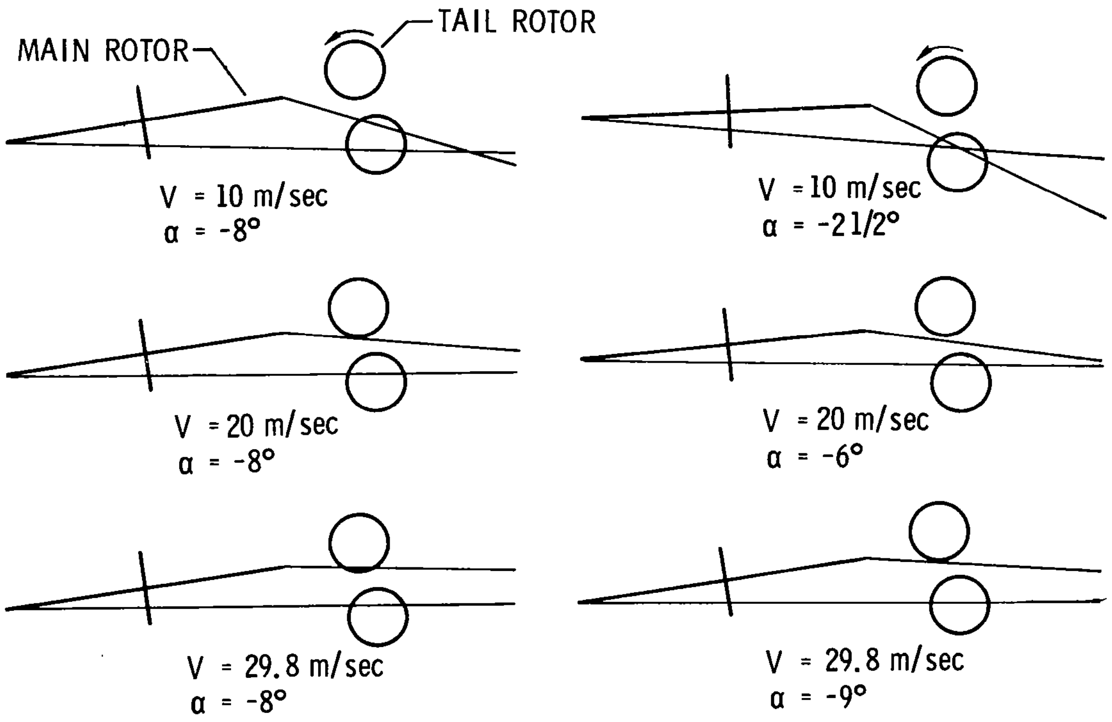

Figure 2.- Calculated wake trajectories.

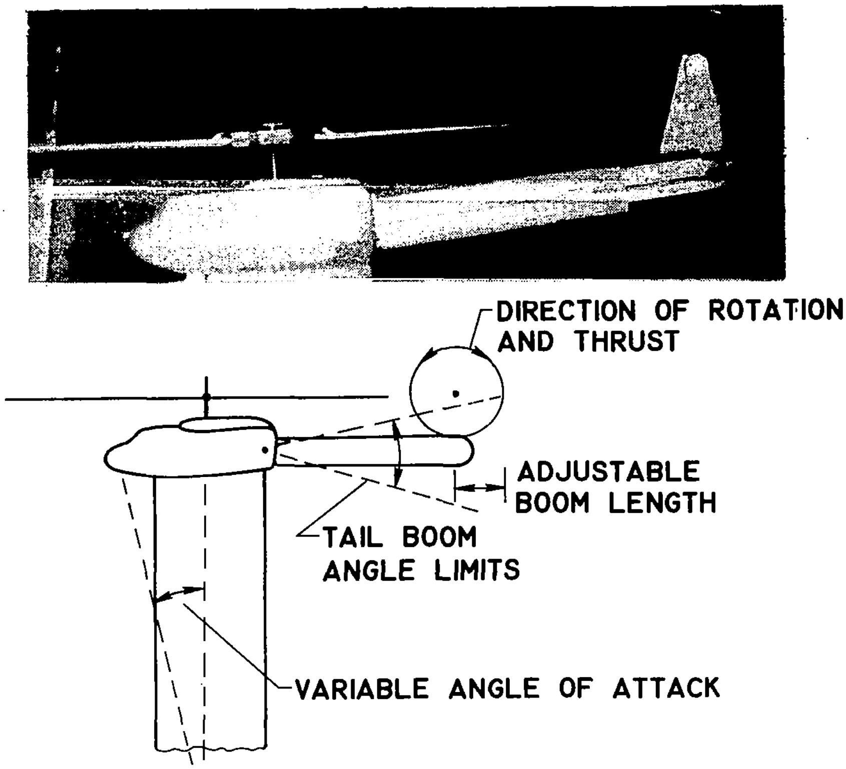

Figure 3.- Wind-tunnel model showing configuration variables.

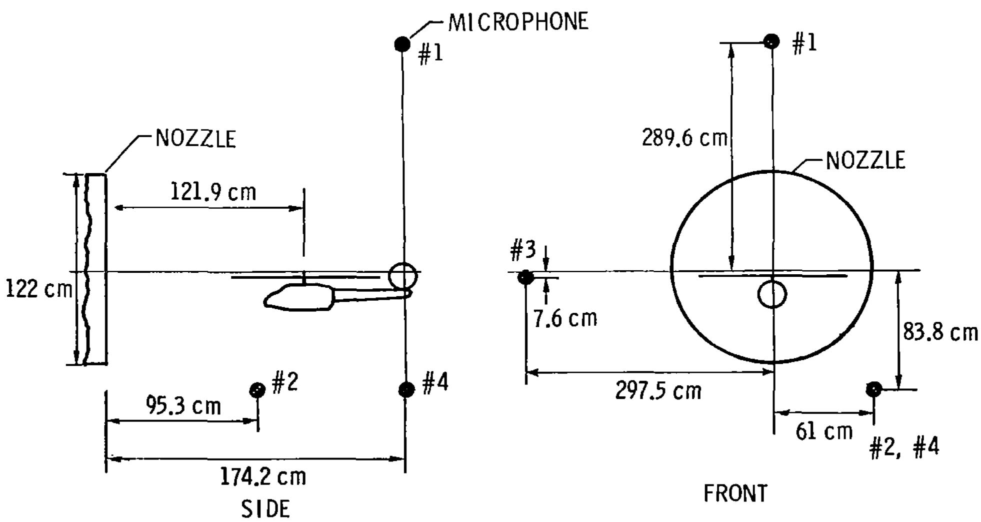

Figure 4.- Microphone locations.

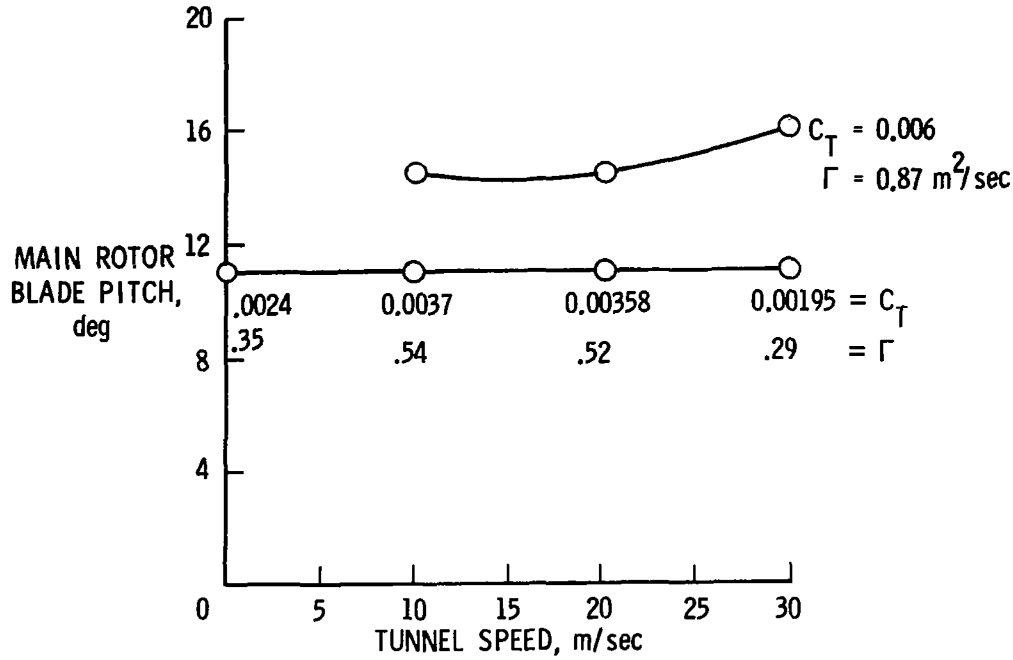

Figure 5.- Model operating conditions.

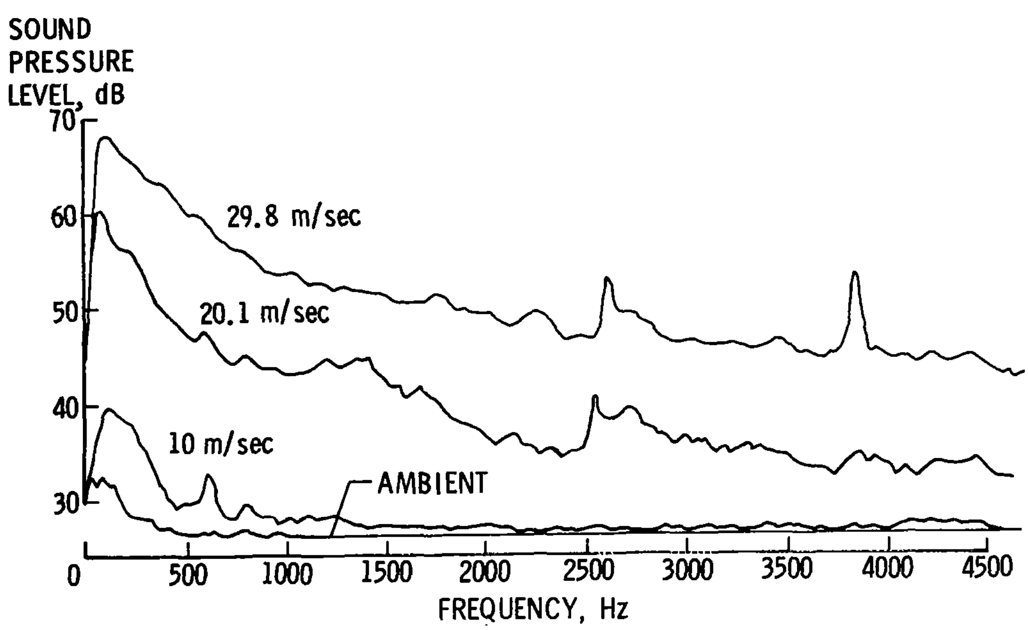

Figure 6.- Anechoic flow facility background noise levels with model installed.

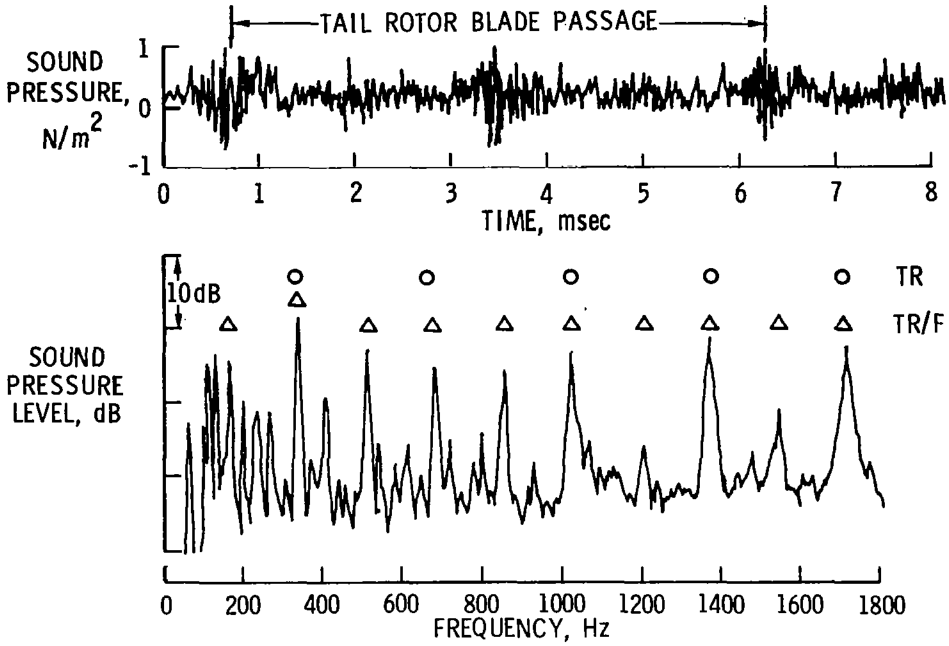

Figure 7.- Typical time history and spectra.

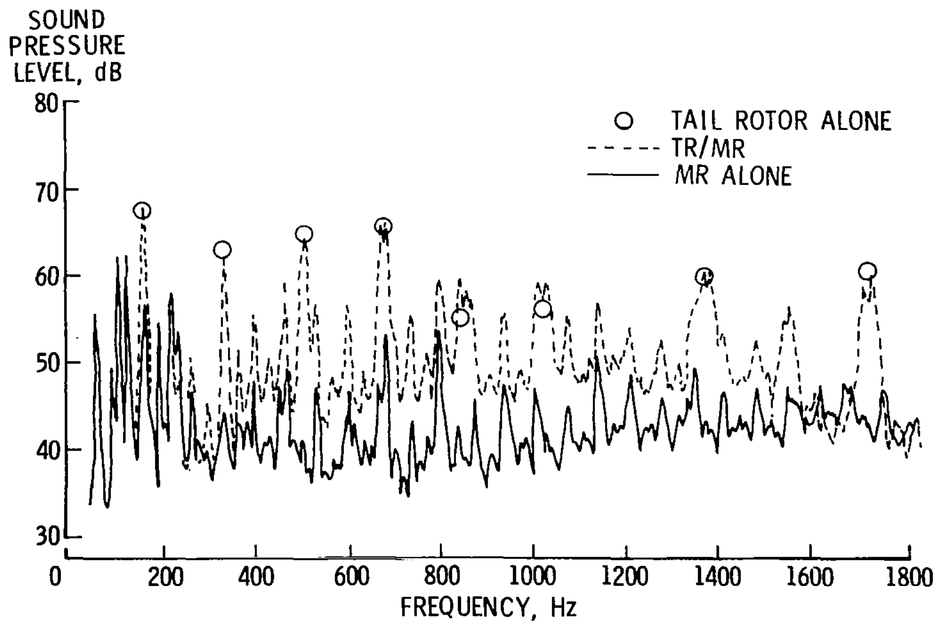

Figure 8.- Hover interaction noise.

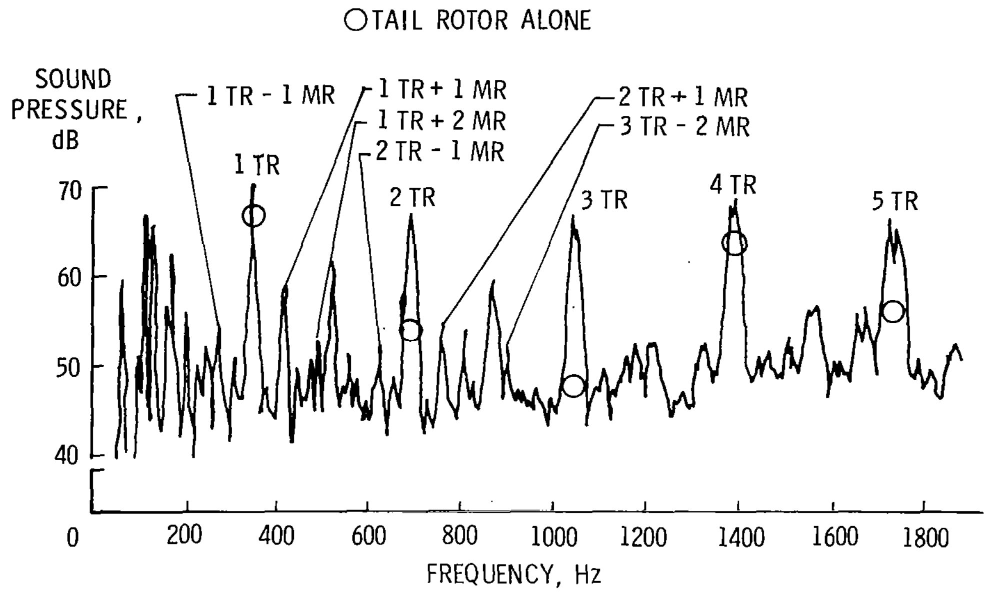

Figure 9.- Tail rotor noise due to main rotr wake interaction. V_{tun} = 10 m/sec.

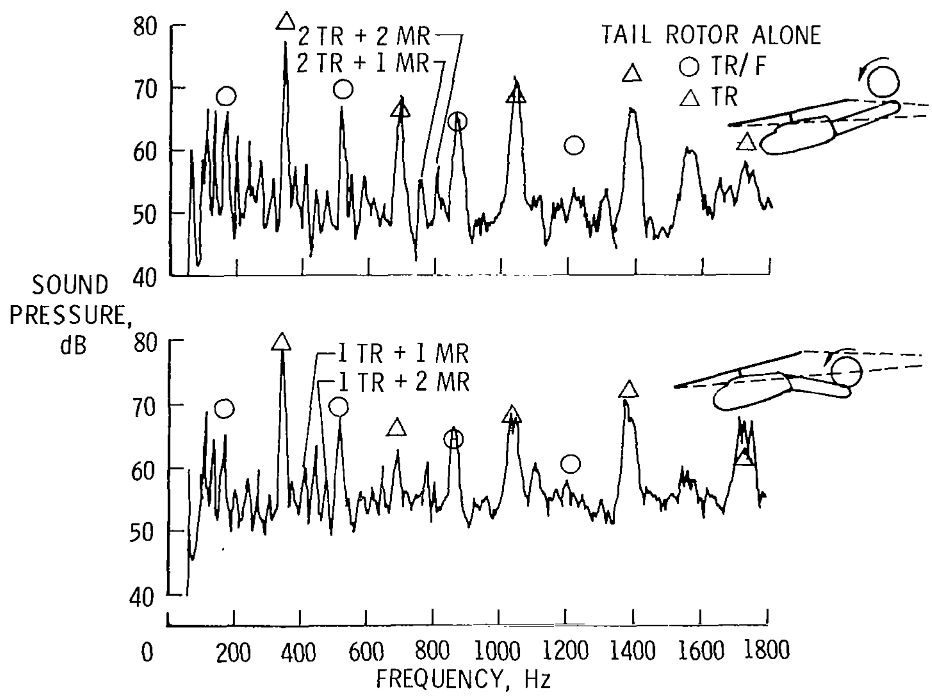

Figure 10.- Tail rotor noise due to main rotor wake interaction. V_{tun} = 20 m/sec.

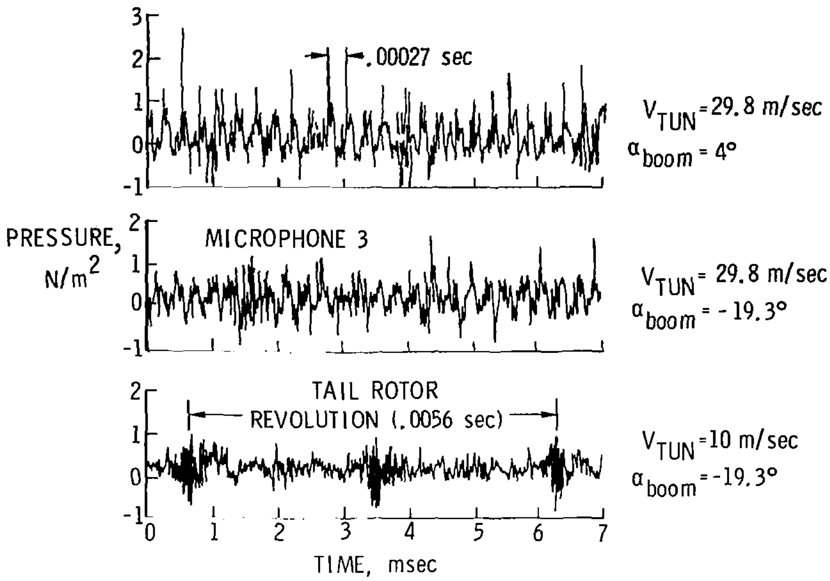

Figure 11.- Acoustic pressure time histories showing vortex intersects.

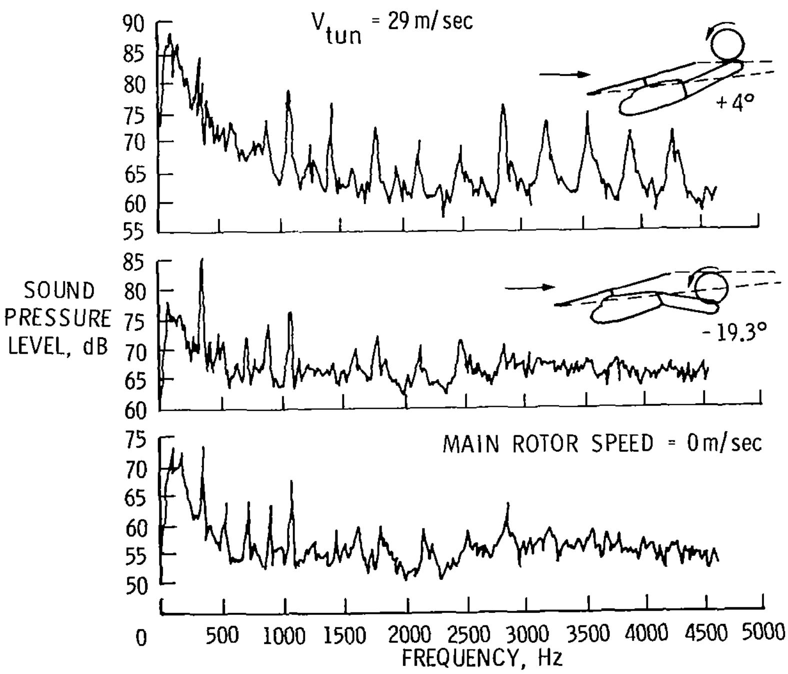

Figure 12.- Effect of tail rotor position on noise.